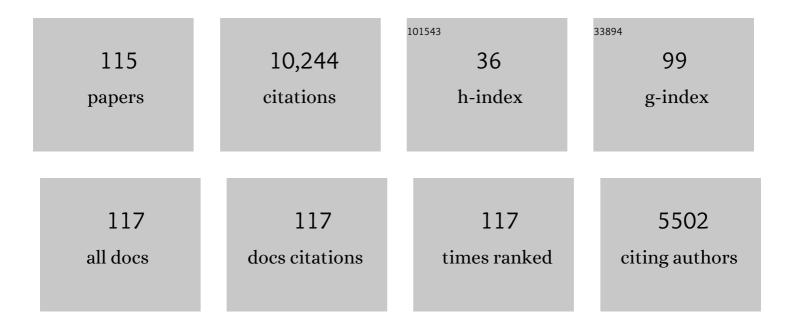
Anton Hohenwarter

List of Publications by Year in descending order

Source: https://exaly.com/author-pdf/2311954/publications.pdf Version: 2024-02-01



#	Article	IF	CITATIONS
1	Microstructure-dependent phase stability and precipitation kinetics in equiatomic CrMnFeCoNi high-entropy alloy: Role of grain boundaries. Acta Materialia, 2022, 223, 117470.	7.9	20
2	Precipitation behavior of a Co-free Fe-Ni-Cr-Mo-Ti-Al maraging steel after severe plastic deformation. Materials Science & Engineering A: Structural Materials: Properties, Microstructure and Processing, 2022, 833, 142416.	5.6	15
3	The beneficial effect of rolling on the fracture toughness and R-curve behavior of pure tungsten. Materials Science & Engineering A: Structural Materials: Properties, Microstructure and Processing, 2022, 838, 142756.	5.6	2
4	Fatigue crack growth of deformed pearlitic rail steels under multiaxial loading. Procedia Structural Integrity, 2022, 39, 313-326.	0.8	3
5	Nanomaterials by severe plastic deformation: review of historical developments and recent advances. Materials Research Letters, 2022, 10, 163-256.	8.7	215
6	Influence of grain aspect-ratio on the fracture properties of ultrafine-grained tantalum. Materials and Design, 2022, 216, 110545.	7.0	4
7	Soft Magnetic Properties of Ultra-Strong and Nanocrystalline Pearlitic Wires. Nanomaterials, 2022, 12, 23.	4.1	3
8	Microstructural Impact on Fatigue Crack Growth Behavior of Alloy 718. Metals, 2022, 12, 710.	2.3	3
9	Deformation-induced medium-range order changes in bulk metallic glasses. Physical Review Materials, 2022, 6, .	2.4	4
10	Achieving 1 GPa fatigue strength in nanocrystalline 316L steel through recovery annealing. Scripta Materialia, 2022, 217, 114773.	5.2	6
11	Crack path investigations in a pearlitic rail steel after pre-deformation under cyclic Mode-II loading. Engineering Failure Analysis, 2022, 140, 106567.	4.0	4
12	Effect of a single overload on the cyclic R-curve behaviour of a Î ³ -TiAl TNM alloy. International Journal of Fatigue, 2022, 163, 107083.	5.7	1
13	High pressure torsion processing of maraging steel 250: Microstructure and mechanical behaviour evolution. Materials Science & Engineering A: Structural Materials: Properties, Microstructure and Processing, 2021, 802, 140665.	5.6	12
14	Extracting information from noisy data: strain mapping during dynamic in situ SEM experiments. Journal of Materials Research, 2021, 36, 2291-2304.	2.6	7
15	Influence of cold rolling on the fatigue crack growth behavior of tungsten. Materials Science & Engineering A: Structural Materials: Properties, Microstructure and Processing, 2021, 805, 140791.	5.6	10
16	Medium-range order dictates local hardness in bulk metallic glasses. Materials Today, 2021, 44, 48-57.	14.2	47
17	The Role of Phase Hardness Differential on the Non-uniform Elongation of a Ferrite-Martensite Dual Phase Steel. Metallurgical and Materials Transactions A: Physical Metallurgy and Materials Science, 2021, 52, 4018-4032.	2.2	10
18	Grain refinement effect on the Ti-45Nb alloy electrochemical behavior in simulated physiological solution. Surface and Coatings Technology, 2021, 423, 127609.	4.8	11

#	Article	IF	CITATIONS
19	Quasi-static and dynamic fracture toughness of a γ-TiAl alloy: Measurement techniques, fractography and interpretation. Engineering Fracture Mechanics, 2021, 258, 108081.	4.3	9
20	Mechanical Behavior and In Vitro Corrosion of Cubic Scaffolds of Pure Magnesium Processed by Severe Plastic Deformation. Metals, 2021, 11, 1791.	2.3	8
21	Fracture of severely plastically deformed titanium. Materials Letters, 2021, 309, 131382.	2.6	1
22	Microstructure and Failure Characteristics of Nanostructured Molybdenum–Copper Composites. Advanced Engineering Materials, 2020, 22, 1900474.	3.5	2
23	On the Room-Temperature Mechanical Properties of an Ion-Irradiated TiZrNbHfTa Refractory High Entropy Alloy. Jom, 2020, 72, 130-138.	1.9	34
24	Microstructures, Mechanical Properties, and Corrosion Behaviors of Refractory High-Entropy ReTaWNbMo Alloys. Journal of Materials Engineering and Performance, 2020, 29, 399-409.	2.5	13
25	Microstructure, strength and fracture toughness of CuNb nanocomposites processed with high pressure torsion using multi-sector disks. Scripta Materialia, 2020, 189, 48-52.	5.2	4
26	Corrosion in Hank's Solution and Mechanical Strength of Ultrafineâ€Grained Pure Iron. Advanced Engineering Materials, 2020, 22, 2000183.	3.5	7
27	Microstructure, Texture, and Strength Development during High-Pressure Torsion of CrMnFeCoNi High-Entropy Alloy. Crystals, 2020, 10, 336.	2.2	39
28	An SEM compatible plasma cell for <i>in situ</i> studies of hydrogen-material interaction. Review of Scientific Instruments, 2020, 91, 043705.	1.3	13
29	Evaluation of the intergranular crack growth resistance of ultrafine grained tungsten materials. Acta Materialia, 2019, 176, 330-340.	7.9	17
30	Nanostructured Metallic Materials and Composites: Processes, Properties and Microstructures. Advanced Engineering Materials, 2019, 21, 1801073.	3.5	0
31	Optimizing mechanical properties of Fe26.7Co26.7Ni26.7Si8.9B11 high entropy alloy by inducing hypoeutectic to quasi-duplex microstructural transition. Scientific Reports, 2019, 9, 360.	3.3	9
32	Tailoring bimodal grain size structures in nanocrystalline compositionally complex alloys to improve ductility. Materials Science & Engineering A: Structural Materials: Properties, Microstructure and Processing, 2019, 748, 379-385.	5.6	54
33	Fracture properties of ultrafine grain chromium correlated to single dislocation processes at room temperature. Journal of Materials Research, 2019, 34, 2370-2383.	2.6	14
34	Influence of annealing on microstructure and mechanical properties of ultrafine-grained Ti45Nb. Materials and Design, 2019, 179, 107864.	7.0	19
35	On the onset of deformation twinning in the CrFeMnCoNi high-entropy alloy using a novel tensile specimen geometry. Intermetallics, 2019, 110, 106469.	3.9	21
36	Electron Irradiation Effects on Strength and Ductility of Polymer Foils Studied by Femtosecond Laser-Processed Micro-Tensile Specimens. Materials, 2019, 12, 1468.	2.9	7

#	Article	IF	CITATIONS
37	Anisotropy in fracture and fatigue resistance of pearlitic steels and its effect on the crack path. International Journal of Fatigue, 2019, 124, 528-536.	5.7	14
38	Anisotropy of Tensile and Fracture Behavior of Pure Titanium after Hydrostatic Extrusion. Materials Transactions, 2019, 60, 2160-2167.	1.2	11
39	Sample Size and Strain-Rate-Sensitivity Effects on the Homogeneity of High-Pressure Torsion Deformed Disks. Metallurgical and Materials Transactions A: Physical Metallurgy and Materials Science, 2019, 50, 601-608.	2.2	18
40	Fatigue Crack-Growth Properties of SPD-Metals. Structural Integrity, 2019, , 347-349.	1.4	1
41	Introduction of Planar High Pressure Torsion (Pâ€HPT) for Fabrication of Nanostructured Sheets. Advanced Engineering Materials, 2018, 20, 1800050.	3.5	12
42	Electrochemical and biocompatibility examinations of highâ€pressure torsion processed titanium and T i–13 N b–13 Z r alloy. Journal of Biomedical Materials Research - Part B Applied Biomaterials, 2018, 106, 1097-1107.	3.4	13
43	Influence of severe plastic deformation and specimen orientation on the fatigue crack propagation behavior of a pearlitic steel. Materials Science & Engineering A: Structural Materials: Properties, Microstructure and Processing, 2018, 710, 260-270.	5.6	27
44	Crack path identification in a nanostructured pearlitic steel using atom probe tomography. Scripta Materialia, 2018, 142, 66-69.	5.2	13
45	Thermodynamic instability of a nanocrystalline, single-phase TiZrNbHfTa alloy and its impact on the mechanical properties. Acta Materialia, 2018, 142, 201-212.	7.9	196
46	Gradient residual strain and stress distributions in a high pressure torsion deformed iron disk revealed by high energy X-ray diffraction. Scripta Materialia, 2018, 146, 178-181.	5.2	20
47	The corrosion resistance in artificial saliva of titanium and Ti-13Nb-13Zr alloy processed by high pressure torsion. Procedia Structural Integrity, 2018, 13, 1834-1839.	0.8	4
48	Effect of processing temperature on the microstructural characteristics of Cu-Ag nanocomposites: From supersaturation to complete phase decomposition. Acta Materialia, 2018, 154, 33-44.	7.9	19
49	Influence of Annealing on Microstructure and Mechanical Properties of a Nanocrystalline CrCoNi Medium-Entropy Alloy. Materials, 2018, 11, 662.	2.9	48
50	Influence of Secondary Phase on Intrinsic Threshold and Path of Shear-Mode Fatigue Cracks in Metals. Acta Physica Polonica A, 2018, 134, 699-702.	0.5	3
51	Structural anisotropy in equal-channel angular extruded nickel revealed by dilatometric study of excess volume. International Journal of Materials Research, 2017, 108, 81-88.	0.3	8
52	Fatigue crack closure: a review of the physical phenomena. Fatigue and Fracture of Engineering Materials and Structures, 2017, 40, 471-495.	3.4	225
53	The use of femtosecond laser ablation as a novel tool for rapid micro-mechanical sample preparation. Materials and Design, 2017, 121, 109-118.	7.0	92
54	Microstructure and texture evolution during severe plastic deformation of CrMnFeCoNi high-entropy alloy. IOP Conference Series: Materials Science and Engineering, 2017, 194, 012028.	0.6	24

#	Article	IF	CITATIONS
55	Effect of temperature on the fatigue-crack growth behavior of the high-entropy alloy CrMnFeCoNi. Intermetallics, 2017, 88, 65-72.	3.9	160
56	The effect of severe grain refinement on the damage tolerance of a superelastic NiTi shape memory alloy. Journal of the Mechanical Behavior of Biomedical Materials, 2017, 71, 337-348.	3.1	22
57	Fatigue crack growth anisotropy in ultrafine-grained iron. Acta Materialia, 2017, 126, 154-165.	7.9	33
58	Phase Decomposition of a Singleâ€Phase AlTiVNb Highâ€Entropy Alloy after Severe Plastic Deformation and Annealing. Advanced Engineering Materials, 2017, 19, 1600674.	3.5	36
59	Fracture of severely plastically deformed Ta and Nb. International Journal of Refractory Metals and Hard Materials, 2017, 64, 143-150.	3.8	6
60	Influence of testing orientation on mechanical properties of Ti45Nb deformed by high pressure torsion. Materials and Design, 2017, 114, 40-46.	7.0	22
61	Femtosecond laser machining for characterization of local mechanical properties of biomaterials: a case study on wood. Science and Technology of Advanced Materials, 2017, 18, 574-583.	6.1	16
62	Impact of severe plastic deformation on microstructure and fracture toughness evolution of a duplex-steel. Materials Science & Engineering A: Structural Materials: Properties, Microstructure and Processing, 2017, 703, 173-179.	5.6	16
63	Insights into the deformation behavior of the CrMnFeCoNi high-entropy alloy revealed by elevated temperature nanoindentation. Journal of Materials Research, 2017, 32, 2658-2667.	2.6	40
64	Internal stress and defect-related free volume in submicrocrystalline Ni studied by neutron diffraction and difference dilatometry. Philosophical Magazine Letters, 2017, 97, 450-458.	1.2	3
65	Simultaneous enhancement of strength and fatigue crack growth behavior of nanocrystalline steels by annealing. Scripta Materialia, 2017, 139, 39-43.	5.2	19
66	Prediction of effective mode II fatigue crack growth threshold for metallic materials. Engineering Fracture Mechanics, 2017, 174, 117-126.	4.3	9
67	Nanoindentation testing as a powerful screening tool for assessing phase stability of nanocrystalline high-entropy alloys. Materials and Design, 2017, 115, 479-485.	7.0	68
68	Strength and ductility of heavily deformed pearlitic microstructures. IOP Conference Series: Materials Science and Engineering, 2017, 219, 012003.	0.6	6
69	Direct measurement of vacancy relaxation by dilatometry. Applied Physics Letters, 2016, 109, .	3.3	16
70	The importance of fracture toughness in ultrafine and nanocrystalline bulk materials. Materials Research Letters, 2016, 4, 127-136.	8.7	82
71	Ultra-strong and damage tolerant metallic bulk materials: A lesson from nanostructured pearlitic steel wires. Scientific Reports, 2016, 6, 33228.	3.3	49
72	Progress in understanding of intrinsic resistance to shear-mode fatigue crack growth in metallic materials. International Journal of Fatigue, 2016, 89, 36-42.	5.7	14

#	Article	IF	CITATIONS
73	Microstructure and metallic ion release of pure titanium and Ti–13Nb–13Zr alloy processed by high pressure torsion. Materials and Design, 2016, 91, 340-347.	7.0	43
74	Anisotropic deformation characteristics of an ultrafine- and nanolamellar pearlitic steel. Acta Materialia, 2016, 106, 239-248.	7.9	82
75	Exceptional damage-tolerance of a medium-entropy alloy CrCoNi at cryogenic temperatures. Nature Communications, 2016, 7, 10602.	12.8	1,175
76	Experimental evidence of a common local mode II growth mechanism of fatigue cracks loaded in modes II, III and II + III in niobium and titanium. International Journal of Fatigue, 2016, 92, 470-477.	5.7	17
77	Deformation and fracture characteristics of ultrafine-grained vanadium. Materials Science & Engineering A: Structural Materials: Properties, Microstructure and Processing, 2016, 650, 492-496.	5.6	12
78	Hardening by annealing: insights from different alloys. IOP Conference Series: Materials Science and Engineering, 2015, 89, 012043.	0.6	18
79	Thermally activated deformation processes in body-centered cubic Cr – How microstructure influences strain-rate sensitivity. Scripta Materialia, 2015, 106, 42-45.	5.2	50
80	Incremental high pressure torsion as a novel severe plastic deformation process: Processing features and application to copper. Materials Science & Engineering A: Structural Materials: Properties, Microstructure and Processing, 2015, 626, 80-85.	5.6	67
81	Mechanical properties, microstructure and thermal stability of a nanocrystalline CoCrFeMnNi high-entropy alloy after severe plastic deformation. Acta Materialia, 2015, 96, 258-268.	7.9	952
82	Fracture and fracture toughness of nanopolycrystalline metals produced by severe plastic deformation. Philosophical Transactions Series A, Mathematical, Physical, and Engineering Sciences, 2015, 373, 20140366.	3.4	60
83	Revisiting fatigue crack growth in various grain size regimes of Ni. Materials Science & Engineering A: Structural Materials: Properties, Microstructure and Processing, 2015, 646, 294-305.	5.6	41
84	Increasing the strength of nanocrystalline steels by annealing: Is segregation necessary?. Scripta Materialia, 2015, 95, 27-30.	5.2	89
85	Analysis of fatigue crack propagation under mixed mode II+III in ARMCO iron. International Journal of Fatigue, 2015, 76, 47-52.	5.7	22
86	Load history effects on fatigue crack propagation: Its effect on the R-curve for threshold. Frattura Ed Integrita Strutturale, 2015, 9, 209-214.	0.9	3
87	Effects of microstructure and crystallography on crack path and intrinsic resistance to shear-mode fatigue crack growth. Frattura Ed Integrita Strutturale, 2015, 9, .	0.9	1
88	Propagation of Long Fatigue Cracks under Remote Modes II and III in Ferritic-Pearlitic Steel. Acta Physica Polonica A, 2015, 128, 611-614.	0.5	0
89	A novel laboratory test rig for probing the sensitivity of rail steels to RCF and wear – first experimental results. Wear, 2014, 316, 101-108.	3.1	11
90	Nearâ€threshold behaviour of shearâ€mode fatigue cracks in metallic materials. Fatigue and Fracture of Engineering Materials and Structures, 2014, 37, 232-254.	3.4	68

#	Article	IF	CITATIONS
91	Influence of heat treatment on the microstructural evolution of Al–3 wt.% Cu during high-pressure torsion. Philosophical Magazine Letters, 2014, 94, 342-350.	1.2	14
92	A fracture-resistant high-entropy alloy for cryogenic applications. Science, 2014, 345, 1153-1158.	12.6	3,982
93	3D Morphology of Fracture Surfaces Created by Mixed-mode II+III Fatigue Loading in Metallic Materials. Procedia Engineering, 2014, 74, 74-77.	1.2	3
94	Fatigue Crack Growth Behavior of Ultrafine-grained Nickel Produced by High Pressure Torsion. , 2014, 3, 1044-1049.		7
95	Direct evidence for grain boundary motion as the dominant restoration mechanism in the steady-state regime of extremely cold-rolled copper. Acta Materialia, 2014, 77, 401-410.	7.9	52
96	Grain boundary excess volume and defect annealing of copper after high-pressure torsion. Acta Materialia, 2014, 68, 189-195.	7.9	51
97	Enhanced fatigue endurance of metallic glasses through a staircase-like fracture mechanism. Proceedings of the National Academy of Sciences of the United States of America, 2013, 110, 18419-18424.	7.1	43
98	Influence of morphology and structural size on the fracture behavior of a nanostructured pearlitic steel. Materials Science & Engineering A: Structural Materials: Properties, Microstructure and Processing, 2013, 585, 190-196.	5.6	35
99	Fracture of ECAP-deformed iron and the role of extrinsic toughening mechanisms. Acta Materialia, 2013, 61, 2973-2983.	7.9	60
100	Three-dimensional morphology of fracture surfaces generated by modes II and III fatigue loading in ferrite and austenite. Engineering Fracture Mechanics, 2013, 108, 285-293.	4.3	20
101	Near-threshold propagation of mode II and mode III fatigue cracks in ferrite and austenite. Acta Materialia, 2013, 61, 4625-4635.	7.9	30
102	Influence of grain shape and orientation on the mechanical properties of high pressure torsion deformed nickel. Materials Science & Engineering A: Structural Materials: Properties, Microstructure and Processing, 2013, 560, 224-231.	5.6	32
103	Cyclic Deformation Behavior of a 316L Austenitic Stainless Steel Processed by High Pressure Torsion. Advanced Engineering Materials, 2012, 14, 948-954.	3.5	18
104	A comprehensive study on the damage tolerance of ultrafine-grained copper. Materials Science & Engineering A: Structural Materials: Properties, Microstructure and Processing, 2012, 540, 89-96.	5.6	40
105	Fracture toughness evaluation of ultrafine-grained nickel. Scripta Materialia, 2011, 64, 982-985.	5.2	80
106	Effect of Large Shear Deformations on the Fracture Behavior of a Fully Pearlitic Steel. Metallurgical and Materials Transactions A: Physical Metallurgy and Materials Science, 2011, 42, 1609-1618.	2.2	72
107	The ductile to brittle transition of ultrafine-grained Armco iron: an experimental study. Journal of Materials Science, 2010, 45, 4805-4812.	3.7	45
108	Anisotropic fracture behavior of ultrafine-grained iron. Materials Science & Engineering A: Structural Materials: Properties, Microstructure and Processing, 2010, 527, 2649-2656.	5.6	64

#	Article	IF	CITATIONS
109	An Overview on the Fracture Behavior of Metals Processed by High Pressure Torsion. Materials Science Forum, 2010, 667-669, 671-676.	0.3	4
110	Saturation of Fragmentation During Severe Plastic Deformation. Annual Review of Materials Research, 2010, 40, 319-343.	9.3	460
111	Technical parameters affecting grain refinement by high pressure torsion. International Journal of Materials Research, 2009, 100, 1653-1661.	0.3	159
112	New procedure to generate stable nanocrystallites by severe plastic deformation. Scripta Materialia, 2009, 61, 1016-1019.	5.2	74
113	Strain effects on the coarsening and softening of electrodeposited nanocrystalline Ni subjected to high pressure torsion. Scripta Materialia, 2008, 58, 790-793.	5.2	39
114	Ultimate Strength of a Tungsten Heavy Alloy after Severe Plastic Deformation at Quasi-Static and Dynamic Loading. Materials Science Forum, 0, 584-586, 405-410.	0.3	14
115	Advantages and Limitations of HPT: A Review. Materials Science Forum, 0, 584-586, 16-21.	0.3	115